TDEM by FDEM

Wim A. Mulder[1, 2] **and Evert C. Slob**[2]

[1] Shell International Exploration and Production B.V., P.O. Box 60, 2280AB Rijswijk, The Netherlands
[2] Delft University of Technology, Faculty of Civil Engineering and Geosciences
Department of Geotechnology, P.O. Box 5028, 2600GA Delft, The Netherlands

Abstract— Time-domain electromagnetic measurements of induction currents are useful for geophysical prospecting in shallow sea water and on land. We review the complexity of several numerical modelling schemes. A multigrid solver makes frequency-domain modelling followed by a Fourier transform an appealing choice. Examples are included.

Controlled-source electromagnetic measurements of induction currents in the earth can provide resistivity maps for geophysical prospecting. In marine environments, the current source often employs one or a few frequencies. In shallow sea water or on land, the response of air is dominant and time-domain measurements are more appropriate. Because electromagnetic signals in the earth are strongly diffusive, direct interpretation of measured data can be difficult. Inversion of the data for a resistivity model may provide better results. Therefore, an efficient modelling and inversion algorithm is required. In the frequency domain, the multigrid method allows for a reasonably fast solution of the discretized equations [1, 2]. On equidistant or mildly stretched grids, the number of iterations required to solve the equations at a given frequency is about 10, independent of the number of unknowns. Only with stronger stretching does the number of iterations increase. A more powerful method based on semi-coarsening and line-relaxation [3] is less sensitive to grid stretching but the required computer time per iteration is much larger. For time-domain modelling, there are a number of methods. The simplest is explicit time stepping, but this is rather costly. The Du Fort-Frankel method [4] is more efficient, but involves an artificial light speed term. Implicit methods are only efficient if a fast solver is available. Drushkin and Knizhnerman [5, 6] proposed a technique based on Lanczos reduction and matrix exponentials. Time-domain solutions can also be obtained from a frequency-domain code after a Fourier transform. An example for horizontally layered media can be found in, for instance, [7].

Here, the computational cost of these methods is compared by complexity analysis. This provides an estimate of the cost as a function of the number of unknowns, but without the actual constants. The next section compares the various methods. The frequency-domain method appears to be attractive. Examples that highlight some of the issues when using a frequency-domain method are included.

1. COMPLEXITY

Numerical modelling of transient EM signals can be performed by various methods. Here we consider an explicit time-stepping scheme, the Du Fort-Frankel method, implicit schemes, matrix exponentials and Lanczos reduction, and Fourier transformed frequency-domain solutions. Complexity analysis provides cost estimates in terms of the number of unknowns, without the constants that determine the actual computer run-time. The latter strongly depend on implementation and hardware details.

The method that is the simplest to implement is the explicit scheme. Unfortunately, this is only stable if the time step $\Delta t \leq ch^2$, where c is a constant depending on the material properties and the discretization, and h is the smallest grid spacing used in the problem. For a three-dimensional problem with n the number of grid points in each coordinate, the spacing $h = O(1/n)$ and the cost of a single time step is $O(n^3)$, so the overall complexity for computing the solution over a given time span T is $O(n^3 T/\Delta t) = O(n^5)$. In practice, this is too slow for practical purposes, except perhaps on massively parallel computers.

The Du Fort-Frankel method [4] offers one way to get around the restrictive stability limit. An artificial light-speed is introduced with size $h/(\Delta t\sqrt{2})$ that allows the time step to grow with the square root of time, without doing too much harm to the accuracy of the solution. Geophysical applications of this method to TDEM problems can be found in, for instance, Oristaglio and Hohmann [8] for the 2D case and Commer and Newman [9] for 3D problems. The cost of the method is of $O(n^4)$.

An implicit scheme can avoid the $O(h^2)$ stability limit as well. The price paid is the solution of a large sparse linear system, which may be costly. An efficient iterative solution method for the frequency-domain equations [1–3] can also be used to solve the time-domain equations at an $O(n^3)$ cost per time step if the grid stretching is sufficiently mild. Together with a time step that scales with the square root of time, this method has the same complexity as the Du Fort-Frankel scheme, although the cost per step will be larger by at least an order of magnitude because of the work required by iterative solver. The method does not require an artificial light-speed term, which may allow for larger time steps without ruining the accuracy.

Drushkin and Knizhnerman [5, 6] proposed a technique that appears to be attractive for 3D applications. The Lanczos method was applied to reduce the original sparse matrix that describes the linear problem to a dense but much smaller one. This small matrix was used to quickly compute the time evolution using matrix exponentials.

The Lanczos method constructs the small matrix iteratively. Drushkin and Knizhnerman [5] show that accurate results can be obtained by performing m iterations, where $m = O(n\sqrt{T \log n})$. Here T is the length of time for which the solution needs to be computed, and n is the number of grid points in one of the spatial coordinates. Because the number of non-zero elements of A for a 3D problem is $O(n^3)$, the cost of the Lanczos decomposition will be of order $n^4\sqrt{\log n}$ for a given length of time T.

Time-domain solutions can be computed by first selecting a number of frequencies, then solving the frequency-domain problem at those frequencies, and finally performing an inverse Fourier transform to the time domain. For n_f frequencies and with an efficient solver that requires $O(1)$ iterations, the complexity is $O(n_f n^3)$, which can be favourable if n_f is small relative to n.

Comparison of the above methods shows that three of them have an asymptotic complexity of $O(n^4)$: the method based on Lanczos reduction, ignoring a logarithmic factor, the Du Fort-Frankel method, and an implicit scheme using an optimal solver with $O(1)$ complexity. The application of a frequency-domain method with the same solver results in an $O(n_f n^3)$ complexity, which may be better if n_f can be small relative to n.

These are only asymptotic results. In practice, the performance will depend on the details of the implementation and the actual constants in the complexity estimates.

The choice of grid is another topic. Diffusion problems have length scaling with the square-root of time. This implies that accurate modelling of a problem with a point-like source in space and time requires an initial grid that is very fine close to the source and gradually becomes less fine. Adaptive grid refinement will accomplish this, but leads to complicated software. Also, the Lanczos decomposition cannot be easily used with dynamic adaptive grid refinement. In the Fourier domain, the computational grid should depend on the skin depth and therefore on the frequency. Each frequency requires a different grid, but that is easier accomplished than time-dependent adaptive local grid refinement.

Although it remains to be seen which of the four methods requires the least computer time for a given accuracy, the frequency-domain approach appears to be quite attractive. Examples that highlight some of the issues in that approach will be presented next.

2. EXAMPLES

The Maxwell equations and Ohm's law for conducting media in the frequency domain can be written as

$$\imath\omega\mu_0\tilde{\sigma}\hat{\mathbf{E}} - \nabla \times \mu_r^{-1}\nabla \times \hat{\mathbf{E}} = -\imath\omega\mu_0\hat{\mathbf{J}}_s.$$

The vector $\hat{\mathbf{E}}(\omega, \mathbf{x})$ represents the electric field components as a function of angular frequency ω and position $\mathbf{x}$. The current source is $\hat{\mathbf{J}}_s(\omega, \mathbf{x})$. The quantity $\tilde{\sigma}(\mathbf{x}) = \sigma - \imath\omega\epsilon_0\epsilon_r$, with $\sigma(\mathbf{x})$ the conductivity, $\epsilon_r(\mathbf{x})$ the relative permittivity, $\mu_r(\mathbf{x})$ the relative permeability, and ϵ_0 and μ_0 their vacuum values. We use the Fourier convention $\mathbf{E}(t, \mathbf{x}) = \frac{1}{2\pi}\int_{-\infty}^{\infty}\hat{\mathbf{E}}(\omega, \mathbf{x})e^{-\imath\omega t}d\omega$.

The first example is a point current source $J_s = \mathbf{j}_s\delta(\mathbf{x})\delta(t)$, $\mathbf{j}_s = (1, 0, 0)^{\mathrm{T}}\,\mathrm{A\,m}$, in a homogeneous formation with a conductivity of $\sigma = 1\,\mathrm{S/m}$. The frequency-domain solutions were computed on a grid which was adapted to the skin depth and finest near the source. For each frequency, the grid was different. Fig. 1 shows the real and imaginary parts of E_1, the x-component of the electric field. Its modulus is included. Frequencies were initially chosen as $10^q\,\mathrm{Hz}$, with q ranging from -2 to 2.25 with an increment of 0.25. To capture the variations, more frequencies were inserted between $q = -1$ and 1 at an increment of 0.125.

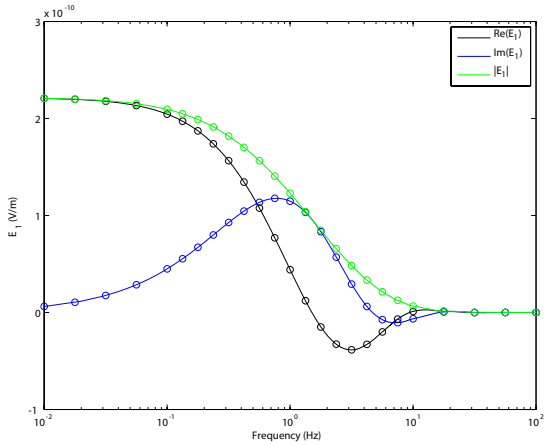

Figure 1: Real and imaginary part and the modulus of E_1 for various frequencies. The circles indicate the computed values, the lines were determined by shape-preserving piecewise cubic interpolation.

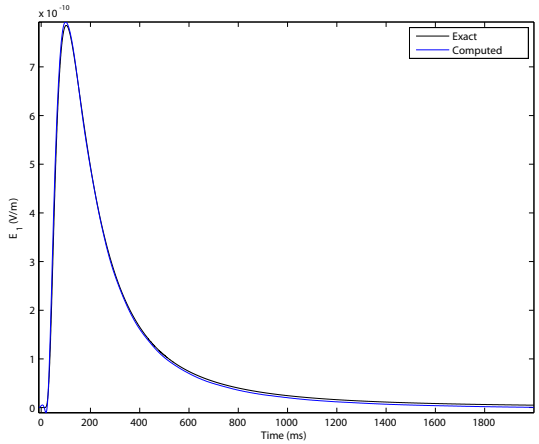

Figure 2: Time-domain solution for the homogeneous problem. Shown in blue is the horizontal component of the electric field. The exact solution is drawn in black.

The data points were interpolated by piecewise cubic Hermite interpolation [11] to an equidistant grid of frequencies and transformed to time. A comparison to the exact solution (see, e.g., [10]) is shown in Figs. 2 and 3. The error are largest at early and late times, due to lack of the lowest and highest frequencies.

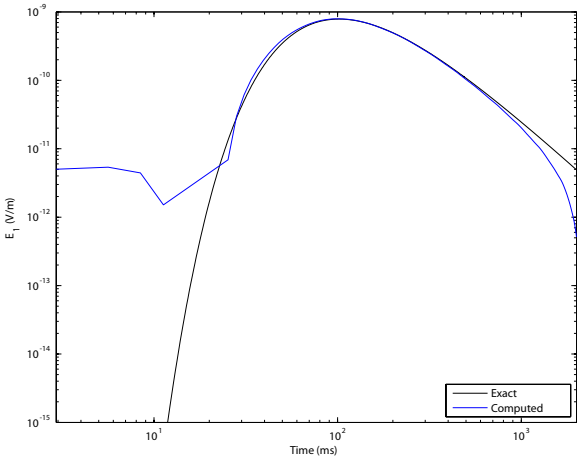

Figure 3: The same time-domain solution for the homogeneous problem as in the previous figure, but now on a logarithmic scale. Only the positive values are displayed.

The second example is a conductive scatterer in a homogeneous background with a conductivity of $1\,\mathrm{S/m}$. The rectangular scatterer with $x \in (-300, 300)\,\mathrm{m}$, $y \in (-200, 200)\,\mathrm{m}$, and $z \in (400, 600)\,\mathrm{m}$ has a conductivity of $10\,\mathrm{S/m}$. The source is the same as in the previous example. In this case, we used a primary/secondary formulation in which the homogeneous response is subtracted so that the source term and its singular response is replaced by a source term that involves the exact solution [10].

The frequency-domain solution for a source at the origin and a receiver located at $(900, 0, 0)\,\mathrm{m}$ and computed on grids with 128^3 cells is displayed in the left panel of Fig. 4. For comparison, we have computed the full electric field for the homogeneous medium with the scatterer and subtracted the numerical solution for the homogeneous medium without the scatterer. The difference is shown in the right panel of Fig. 4.

The time-domain response is shown in Fig. 5 next to the exact homogeneous solution.

In the examples, frequencies were selected on a logarithmic scale and more were added where needed. The grid was based on the skin depth and was different for each frequency. Solutions were

obtained in 8 iterations for the higher frequencies. However, several hundreds of iterations were required at 0.01 Hz, where strong grid stretching was required to include the small scatterer and have an outer boundary sufficiently far away. This calls for a better solver, for instance, the one described in [3].

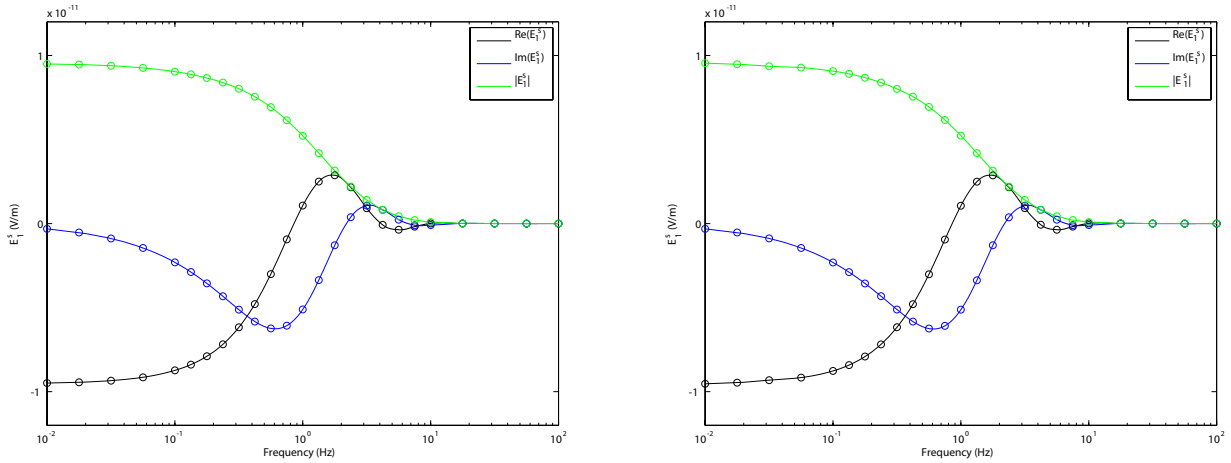

Figure 4: The left figure shows the secondary solution in the frequency domain computed for grids with 128^3 cells. At the right, solutions obtained by taking the difference between the full solutions with and without scatterer is plotted.

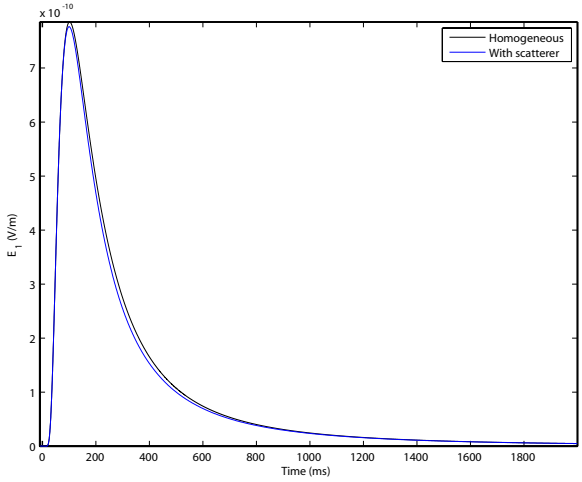

Figure 5: The time-domain solution for the scatterer computed with the primary/secondary formulation on a grid with 128^3 cells. The exact solution for the homogeneous case is shown in black for comparison.

A realistic geophysical model was considered in [2]. Here we use the same model, but without adding an extra 500 m of sea water, so the sea is fairly shallow. Fig. 6 displays the resistivity on a logarithmic scale. Initial solutions for computed at frequencies 10^q Hz, with q between -2.75 and 2.5 at a 0.25 increment. Next, frequencies were added by comparing receiver values at a given frequency to results obtained by interpolation without including that frequency. If the difference between the interpolated and actual value exceeded a tolerance, extra frequencies were added. This was repeated a few times. Cubic interpolation or extrapolation of solutions for other frequencies was use to obtain an initial guess for the iterative solution method. The spatial grid was again based on a balance between the skin depth at the given frequency and the details of the model. One of the time-domain solutions is shown in Fig. 7. The air-wave shows up as an early peak. The anti-causal part must be caused by missing high frequencies and numerical errors.

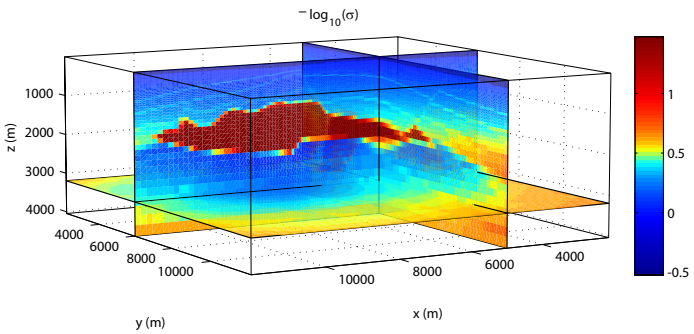

Figure 6: Resistivity model with a highly resistive salt body.

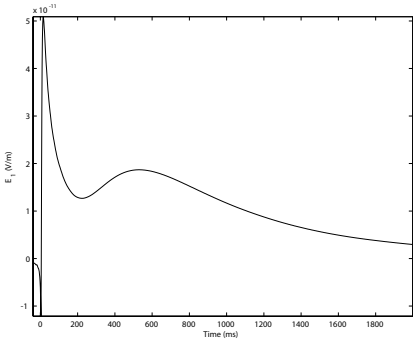

Figure 7: Time response for E_1, for a source at (6500,6500,50) m and a receiver at (9000,6500,100) m at the sea bottom.

3. CONCLUSIONS

Complexity analysis of time-domain methods for modelling electromagnetic diffusion shows that some common methods have an $O(n^4)$ complexity, where n is the number of points per spatial coordinate. Synthesizing time-domain solutions by using a frequency-domain method has a complexity of $O(n_f n^3)$, with n_f the number of frequencies, if the solver convergences in a fixed number of iterations. This can be accomplished by multigrid on uniform or mildly stretched grids. When n_f is small relative to n, this frequency-domain method appears to be the most appealing. However, as our complexity analysis only provides estimates in terms of the number of unknowns and the actual required computer time will also depend on the constants in the estimates, a true comparison of methods should involve the operation count or the cpu-time measured for an actual implementation.

Examples were included to show how frequencies can be selected and how time-domain solutions can be obtained by monotone piecewise cubic interpolation and Fourier transforms. A remaining problem is the large number of iterations that the multigrid solver needs when strong grid stretching is required at the very low frequencies.

REFERENCES

1. Mulder, W. A., "A multigrid solver for 3D electromagnetic diffusion," *Geophys. Prosp.*, Vol. 54, 663–649, 2006.
2. Mulder, W. A., "Geophysical modelling of 3D electromagnetic diffusion with multigrid," *Computing and Visualization in Science*, in press, 2006.
3. Jönsthövel, T. B., C. W. Oosterlee, and W. A. Mulder, "Improving multigrid for 3-D electromagnetic diffusion on stretched grids," *Proceedings, ECCOMAS European Conference on Computational Fluid Dynamics*, Egmond aan Zee, The Netherlands, September 2006.
4. Du Fort, E. C. and S. P. Frankel, "Stability conditions on the numerical treatment of parabolic differential equations," *Math. Tables and Other Aids to Comput. (Math. Comp.)*, Vol. 7, 135–152, 1953.
5. Drushkin, V. L. and L. A. Knizhnerman, "Spectral approach to solving three-dimensional Maxwell's diffusion equations in the time and frequency domains," *Radio Science*, Vol. 29, 937–953, 1994.
6. Drushkin, V. L., L. A. Knizhnerman, and P. Lee, "New spectral Lanczos decomposition method for induction modeling in arbitrary 3-D geometry," *Geophysics*, Vol. 64, 701–706, 1999.
7. Newman, G. A., G. W. Hohmann, and W. L. Anderson, "Transient electromagnetic response of a three-dimensional body in a layered earth," *Geophysics*, Vol. 51, 1608–1627, 1986.
8. Oristaglio, M. L. and G. W. Hohmann, "Diffusion of electromagnetic fields into a two-dimensional earth: A finite-difference approach," *Geophysics*, Vol. 49, 870–894, 1984.
9. Commer, M. A. and G. A. Newman, "A parallel finite-difference approach for 3D transient electromagnetic modeling with galvanic sources," *Geophysics*, Vol. 69, 1192–1202, 2004.
10. Ward, S. A. and G. W. Hohmann, "Electromagnetic theory for geophysical applications," *Electromagnetic Methods in Applied Geophysics — Theory*, Vol. 1, 1987.
11. Fritsch, F. N. and R. E. Carlson, "Monotone piecewise cubic interpolation," *SIAM J. Numer. Anal.*, Vol. 17, 238–246, 1980.